# Finite Element Structural Analysis of Local Instability

J. S. PRZEMIENIECKI*
*Air Force Institute of Technology, Wright-Patterson Air Force Base, Ohio*

**A finite element analysis is presented for predicting local buckling stresses in plates, stiffened panels, and thin-walled columns for which the cross section is made up of thin flat plates. The analysis leads to the formulation of the elastic and geometrical stiffness matrices appearing in an eigenvalue equation used to determine the buckling stress. The stiffness matrices are derived from the exact sinusoidal lengthwise variation of displacements. The resulting sinusoidal stiffness matrices depend on the wavelength of the buckled pattern, but this dependence is of a very simple form, since all stiffness coefficients contain the buckling wavelength as a common factor. Examples are given to illustrate application of the method to several typical aircraft structural components.**

## Introduction

THE finite element methods of structural analysis have now become universally accepted in structural design. These methods provide a means for rapid and accurate stress and deflection analysis of complex structures under static and dynamic loading conditions, and they can also be used very effectively for the structural instability analysis. Although both the displacement and force formulations have been used for stability analyses, the displacement formulation is more attractive because it is easier to program for the computer. In the displacement formulation, the structural stability is analyzed by introducing geometrical stiffnesses which are added to elastic stiffnesses to form a combined stiffness matrix. Since the geometrical stiffness matrix depends on the initial, linear stress distribution within the structure, the addition of elastic and geometrical stiffnesses leads to the formulation of equilibrium equations of the standard eigenvalue type from which the buckling stress can be determined.

The basic concept of geometrical stiffness was first used by Turner et al.[1] for the analysis of structures idealized into pin-jointed bars and triangular plates carrying membrane stresses. The method used was essentially based on the strain energy formulation for large deflections. Similar methods have been used by other authors for the stability analysis of finite size structures made up from bars and beam elements, triangular or rectangular plates, and shell elements.[2-10]

In developing the finite element analysis for structural stability, attention has been mainly focused on the over-all stability of structures. However, in designing aircraft or other lightweight structures, it is often necessary to determine the local instability of various structural components such as plates, thin-walled columns or stiffened panels. The cross section of these components is frequently made up of a number of thin flat plates joined edge to edge. The translational stiffness in the plane of a component flat is much greater than the rotational stiffness about the edge lines. It is possible, therefore, to assume that for such thin-walled cross sections no component flat is translated in its own plane during buckling, and that the edge lines at the junctions between flats remain fixed in space. Thus all possible modes of deformation for local buckling consist simply of pivoting of the component flats about their common edge lines. Using this simplifying assumption, analytical solutions can be derived in which the buckling stress is determined from a transcendental equation. In these equations, both the longitudinal half-wavelength and the longitudinal compressive stress appear as unknown variables, and for any assumed value of the half-wavelength there is, in general, an infinite number of values of the stress for which the transcendental equation is satisfied. The correct solution for the half-wavelength is that which minimizes the lowest value of the stress. The general theory for local instability of plates, panels, and thin-walled columns, based on the classical theory of elasticity, was presented by Cox.[11] More recently, Wittrick[12] and Viswanathan et al.[13] presented an extension of the general theory to allow in-plane deformations and derived the basic equations relating the forces and moments to deflections and rotations of the edge lines at the junctions between the component flats. The determinant of the coefficients in these equations, when equated to zero, forms the stability criterion. Since each coefficient in the stability determinant is a transcendental function of both the compressive stress and the longitudinal half-wavelength the computational procedure for obtaining the buckling stress is very time consuming.

In this paper a finite-element method is presented for the analysis of local instability of plates, thin-walled columns, and stiffened panels, such as those shown in Fig. 1 for which the modes of buckling deformation consist of pivoting of the cross-sectional component flats about their common edge lines. Since the longitudinal dimension of the structural components considered here is many times greater than a typical cross-sectional dimension, any standard method of matrix analysis would require a very large number of finite elements, particularly if the cross-sectional geometry is complex. This in turn leads to very large size matrices for the calculation of the lowest eigenvalue representing the buckling stress. In the present paper, the necessity of using a large number of elements is eliminated by making use of the exact lengthwise variation of displacements in order to derive special elastic and geometrical stiffness matrices, both of which depend on the buckling wavelength. This dependence is of a simple form, since all coefficients in the

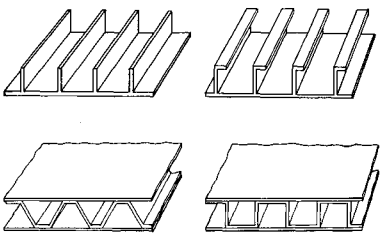

**Fig. 1 Examples of stiffened panels.**

Presented as Paper 72-354 at the AIAA/ASME/SAE 13th Structures, Structural Dynamics, and Materials Conference, San Antonio, Texas, April 10-12, 1972; submitted April 24, 1972; revision received August 7, 1972. The work was partially supported by the Directorate of Science, Air Force Systems Command. The author wishes to acknowledge F. K. Bogner and C. W. Richard for their assistance in preparing the computer program.

Index categories: Aircraft Structural Design (Including Loads); Structural Stability Analysis.

* Dean, School of Engineering. Associate Fellow AIAA.

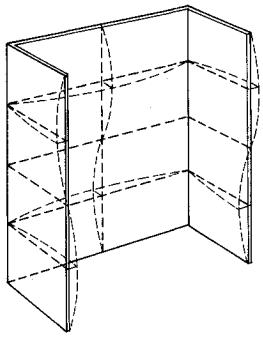

**Fig. 2 Local buckling pattern of a channel-section column.**

resulting stiffness matrices contain the buckling half-wavelength only as a common factor allowing for considerable simplification in any numerical computations. The analysis leads to the standard eigenvalue equation from which the buckling stress is determined by searching for a wavelength corresponding to the lowest value of the buckling stress. Since in practical applications only a very few finite elements are involved, this search is accomplished with a minimum of computational effort. To illustrate this new technique of determining local buckling stresses, several examples of typical aircraft components are included.

## Finite Element Stability Analysis

The finite element stiffness matrices used in the displacement method of stability analysis can be derived most conveniently by starting with the nonlinear strain-displacement equations. These equations can be written in Cartesian coordinates as

$$\begin{aligned}
e_{xx} &= \frac{\partial u_x}{\partial x} + \frac{1}{2}\left[\left(\frac{\partial u_x}{\partial x}\right)^2 + \left(\frac{\partial u_y}{\partial x}\right)^2 + \left(\frac{\partial u_z}{\partial x}\right)^2\right] \\
e_{yy} &= \frac{\partial u_y}{\partial y} + \frac{1}{2}\left[\left(\frac{\partial u_x}{\partial y}\right)^2 + \left(\frac{\partial u_y}{\partial y}\right)^2 + \left(\frac{\partial u_z}{\partial y}\right)^2\right] \\
e_{zz} &= \frac{\partial u_z}{\partial z} + \frac{1}{2}\left[\left(\frac{\partial u_x}{\partial z}\right)^2 + \left(\frac{\partial u_y}{\partial z}\right)^2 + \left(\frac{\partial u_z}{\partial z}\right)^2\right] \\
e_{xy} &= \frac{\partial u_y}{\partial x} + \frac{\partial u_x}{\partial y} + \frac{\partial u_x}{\partial x}\frac{\partial u_x}{\partial y} + \frac{\partial u_y}{\partial x}\frac{\partial u_y}{\partial y} + \frac{\partial u_z}{\partial x}\frac{\partial u_z}{\partial y} \\
e_{yz} &= \frac{\partial u_z}{\partial y} + \frac{\partial u_y}{\partial z} + \frac{\partial u_x}{\partial y}\frac{\partial u_x}{\partial z} + \frac{\partial u_y}{\partial y}\frac{\partial u_y}{\partial z} + \frac{\partial u_z}{\partial y}\frac{\partial u_z}{\partial z} \\
e_{zx} &= \frac{\partial u_x}{\partial z} + \frac{\partial u_z}{\partial x} + \frac{\partial u_x}{\partial z}\frac{\partial u_x}{\partial x} + \frac{\partial u_y}{\partial z}\frac{\partial u_y}{\partial x} + \frac{\partial u_z}{\partial z}\frac{\partial u_z}{\partial x}
\end{aligned} \tag{1}$$

where $u_x$, $u_y$, and $u_z$ represent the displacements in the $x$, $y$, and $z$ directions, respectively. The above strains can be denoted collectively by a column matrix

$$\mathbf{e} = \{e_{xx}\, e_{yy}\, e_{zz}\, e_{xy}\, e_{yz}\, e_{zx}\} \tag{2}$$

which can also be expressed as the sum of linear and nonlinear strains, i.e.

$$\mathbf{e} = \hat{\mathbf{e}} + \mathbf{e}' \tag{3}$$

where $\hat{\mathbf{e}}$ denotes the linear strains while $\mathbf{e}'$ denotes the nonlinear strains.

The displacements $u_x$, $u_y$, and $u_z$ are assumed to be expressible by the equations

$$u_i = \mathbf{a}_i \mathbf{u}; \qquad i = x, y, z \tag{4}$$

where

$$\mathbf{u} = \{u_1 u_2 \ldots u_n\} \tag{5}$$

denotes a column matrix of the finite element displacements (including rotations) and $\mathbf{a}_i$ is a row matrix whose coefficients are, in general, functions of the $x$, $y$, and $z$ coordinates. For some simple finite elements, the matrix $\mathbf{a}_i$ can be determined exactly, while for others assumed displacement distributions must be used in deriving Eq. (4). Substituting Eq. (4) into (1), it follows that

$$\mathbf{e} = \begin{bmatrix} \mathbf{b}_{xx} \\ \mathbf{b}_{yy} \\ \mathbf{b}_{zz} \\ \mathbf{b}_{yx}+\mathbf{b}_{xy} \\ \mathbf{b}_{zy}+\mathbf{b}_{yz} \\ \mathbf{b}_{xz}+\mathbf{b}_{zx} \end{bmatrix} \mathbf{u} + \begin{bmatrix} \frac{\mathbf{b}_{xx}}{2^{1/2}} \\ \frac{\mathbf{b}_{xy}}{2^{1/2}} \\ \frac{\mathbf{b}_{xz}}{2^{1/2}} \\ \mathbf{b}_{xx} \\ \mathbf{b}_{xy} \\ \mathbf{b}_{xz} \end{bmatrix} \mathbf{u} * \begin{bmatrix} \frac{\mathbf{b}_{xx}}{2^{1/2}} \\ \frac{\mathbf{b}_{xy}}{2^{1/2}} \\ \frac{\mathbf{b}_{xz}}{2^{1/2}} \\ \mathbf{b}_{xy} \\ \mathbf{b}_{xz} \\ \mathbf{b}_{xx} \end{bmatrix} \mathbf{u} + \begin{bmatrix} \frac{\mathbf{b}_{yx}}{2^{1/2}} \\ \frac{\mathbf{b}_{yy}}{2^{1/2}} \\ \frac{\mathbf{b}_{yz}}{2^{1/2}} \\ \mathbf{b}_{yx} \\ \mathbf{b}_{yy} \\ \mathbf{b}_{yz} \end{bmatrix} \mathbf{u} * \begin{bmatrix} \frac{\mathbf{b}_{yx}}{2^{1/2}} \\ \frac{\mathbf{b}_{yy}}{2^{1/2}} \\ \frac{\mathbf{b}_{yz}}{2^{1/2}} \\ \mathbf{b}_{yy} \\ \mathbf{b}_{yz} \\ \mathbf{b}_{yx} \end{bmatrix} \mathbf{u} + \begin{bmatrix} \frac{\mathbf{b}_{zx}}{2^{1/2}} \\ \frac{\mathbf{b}_{zy}}{2^{1/2}} \\ \frac{\mathbf{b}_{zz}}{2^{1/2}} \\ \mathbf{b}_{zx} \\ \mathbf{b}_{zy} \\ \mathbf{b}_{zz} \end{bmatrix} \mathbf{u} * \begin{bmatrix} \frac{\mathbf{b}_{zx}}{2^{1/2}} \\ \frac{\mathbf{b}_{zy}}{2^{1/2}} \\ \frac{\mathbf{b}_{zz}}{2^{1/2}} \\ \mathbf{b}_{zy} \\ \mathbf{b}_{zz} \\ \mathbf{b}_{zx} \end{bmatrix} \mathbf{u} \tag{6}$$

where

$$\mathbf{b}_{ij} = \partial \mathbf{a}_i / \partial j; \qquad i, j = x, y, z \tag{7}$$

and asterisks denote element-by-element matrix multiplication. Equation (6) can be expressed in a condensed form as

$$\mathbf{e} = \hat{\mathbf{b}}\mathbf{u} + \sum_i (\mathbf{b}_{i1}\mathbf{u}) * (\mathbf{b}_{i2}\mathbf{u}); \qquad i = x, y, z \tag{8}$$

where $\hat{\mathbf{b}}$ represents linear strains resulting from unit displacements $\mathbf{u}$, while $\mathbf{b}_{i1}$ and $\mathbf{b}_{i2}$ denote the first and second column matrices appearing in the asterisk multiplication products. Hence, from Eqs. (3) and (8) it follows that

$$\hat{\mathbf{e}} = \hat{\mathbf{b}}\mathbf{u} \tag{9}$$

$$\mathbf{e}' = \sum_i (\mathbf{b}_{i1}\mathbf{u}) * (\mathbf{b}_{i2}\mathbf{u}); \qquad i = x, y, z \tag{10}$$

The stresses $\boldsymbol{\sigma}$ are obtained from the Hooke's law

$$\boldsymbol{\sigma} = \mathbf{E}\mathbf{e} \tag{11}$$

where $\mathbf{E}$ represents the matrix of elastic constants. The stress matrix $\boldsymbol{\sigma}$ is then used to determine the strain energy $U$ from the expression

$$U = \tfrac{1}{2}\int_v \mathbf{e}^T \boldsymbol{\sigma}\, dv \tag{12}$$

Using Eqs. (3), (11) and (12), it can be shown that, neglecting the nonlinear strain product $(\mathbf{e}')^T\mathbf{E}\mathbf{e}'$, the strain energy expression becomes

$$U = \tfrac{1}{2}\int_v (\hat{\mathbf{e}}^T\mathbf{E}\hat{\mathbf{e}} + 2\hat{\boldsymbol{\sigma}}^T\mathbf{e}')\, dv \tag{13}$$

where

$$\hat{\boldsymbol{\sigma}} = \mathbf{E}\hat{\mathbf{e}} \tag{14}$$

denotes the linear stress matrix. Subsequent substitution of Eqs. (9) and (10) into strain energy expression (13) finally leads to

$$U = \tfrac{1}{2}\int_v [\mathbf{u}^T\hat{\mathbf{b}}^T\mathbf{E}\hat{\mathbf{b}}\mathbf{u} + 2\sum_i \hat{\boldsymbol{\sigma}}^T(\mathbf{b}_{i1}\mathbf{u}) * (\mathbf{b}_{i2}\mathbf{u})]\, dv \tag{15}$$

Application of Castigliano's theorem (Part I) results in the force-displacement relation of the form

$$\partial U/\partial \mathbf{u} = \mathbf{k}\mathbf{u} = \mathbf{S} \tag{16}$$

where $\mathbf{k}$ represents the finite-element stiffness matrix, while $\mathbf{S}$ represents the element forces corresponding with the displacements $\mathbf{u}$. Performing matrix differentiation on Eq. (15), it can be demonstrated that

$$\mathbf{S} = \partial U/\partial \mathbf{u} = \int_v \hat{\mathbf{b}}^T\mathbf{E}\hat{\mathbf{b}}\, dv\, \mathbf{u} + \int_v \sum_i (\mathbf{b}_{i1}{}^T\hat{\boldsymbol{\sigma}}^D\mathbf{b}_{i2} + \mathbf{b}_{i2}{}^T\hat{\boldsymbol{\sigma}}^D\mathbf{b}_{i1})\, dv\, \mathbf{u} \tag{17}$$

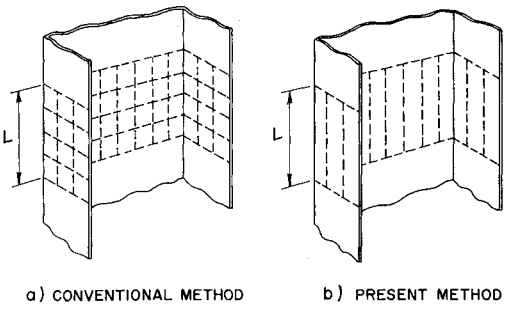


**Fig. 3 Comparison of the finite element strip and conventional idealizations.**

where $\hat{\sigma}^D$ represents the column matrix of stresses $\hat{\sigma}$ changed into a diagonal matrix. It follows, therefore, from Eqs. (16) and (17) that the combined stiffness $\mathbf{k}$ is given by

$$\mathbf{k} = \mathbf{k}_E + \mathbf{k}_G \tag{18}$$

where

$$\mathbf{k}_E = \int_v \hat{\mathbf{b}}^T \mathbf{E} \hat{\mathbf{b}}\, dv \tag{19}$$

represents the element elastic stiffness and

$$\mathbf{k}_G = \int_v \sum_i (\mathbf{b}_{i1}{}^T \hat{\sigma}^D \mathbf{b}_{i2} + \mathbf{b}_{i2}{}^T \hat{\sigma}^D \mathbf{b}_{i1})\, dv \tag{20}$$

represents the element geometrical stiffness. This latter matrix can be simplified further by introducing two new column matrices

$$\mathbf{b}_1 = \{\mathbf{b}_{x1} \mathbf{b}_{y1} \mathbf{b}_{z1}\} \tag{21}$$

and

$$\mathbf{b}_2 = \{\mathbf{b}_{x2} \mathbf{b}_{y2} \mathbf{b}_{z2}\} \tag{22}$$

so that Eq. (20) can be written as

$$\mathbf{k}_G = \int_v (\mathbf{b}_1{}^T \hat{\sigma}_3{}^D \mathbf{b}_2 + \mathbf{b}_2{}^T \hat{\sigma}_3{}^D \mathbf{b}_1)\, dv \tag{23}$$

where

$$\hat{\sigma}_3{}^D = [\hat{\sigma}^D \hat{\sigma}^D \hat{\sigma}^D] \tag{24}$$

In most practical applications, normally only one nonlinear term in the strain-displacement equation is included; the remaining two nonlinear terms are rejected as being of higher order of smallness. For these cases, the matrices $\mathbf{b}_1$ and $\mathbf{b}_2$ are reduced to only one submatrix, $\hat{\sigma}_3{}^D$ becomes $\hat{\sigma}^D$, and the geometrical stiffness matrix is then written as

$$\mathbf{k}_G = \int_v (\mathbf{b}_1{}^T \hat{\sigma}^D \mathbf{b}_2 + \mathbf{b}_2{}^T \hat{\sigma}^D \mathbf{b}_1)\, dv \tag{25}$$

It has therefore been demonstrated that both the elastic and geometrical stiffness matrices for finite elements can be determined from integrals of simple matrix products evaluated over the element volume. Although the derivation presented in this paper has been restricted to Cartesian coordinates, the general method can also be applied to other coordinate systems, e.g. cylindrical coordinate system.

Once the combined stiffness $\mathbf{k}$ has been determined for each finite element, the element stiffness can be transferred into a common (global) displacement system, and the assembled structure stiffness matrix

$$\mathbf{K} = \mathbf{K}_E + \mathbf{K}_G \tag{26}$$

is obtained from the summation of element stiffness. The equations of equilibrium are then formulated as

$$(\mathbf{K}_E + \mathbf{K}_G)\mathbf{U} = \mathbf{P} \tag{27}$$

where $\mathbf{U}$ is a column matrix of node displacements corresponding to the external forces $\mathbf{P}$. The external loading may be expressed as

$$\mathbf{P} = \lambda \mathbf{P}^* \tag{28}$$

where $\lambda$ is a proportionality constant and $\mathbf{P}^*$ represents relative magnitudes of the applied external forces. Also, since the stresses $\hat{\sigma}$ are proportional to the applied loading, the geometrical stiffness matrix can be written as

$$\mathbf{K}_G = \lambda \mathbf{K}_G{}^* \tag{29}$$

where $\mathbf{K}_G{}^*$ is the geometrical stiffness matrix for the reference values of the applied loading. Using, therefore, Eqs. (28) and (29) in Eq. (27), it follows that

$$(\mathbf{K}_E + \lambda \mathbf{K}_G{}^*)\mathbf{U} = \lambda \mathbf{P}^* \tag{30}$$

Hence

$$\mathbf{U} = (\mathbf{K}_E + \lambda \mathbf{K}_G{}^*)^{-1} \lambda \mathbf{P}^* \tag{31}$$

provided the rigid body degrees of freedom are eliminated from $\mathbf{K}_E$ and $\mathbf{K}_G{}^*$.

A perusal of Eq. (31) indicates that the displacements $\mathbf{U}$ will tend to infinity when

$$|\mathbf{K}_E + \lambda \mathbf{K}_G{}^*| = 0 \tag{32}$$

This equation represents the stability determinant for structures idealized into finite elements. The smallest value of $\lambda$ determines the instability condition for a specified loading configuration. In practical applications, however, instead of finding the smallest root of the stability determinant (32), the homogeneous set of equations

$$(\mathbf{K}_E + \lambda \mathbf{K}_G{}^*)\mathbf{U} = \mathbf{0} \tag{33}$$

is used to determine the eigenvalues by means of any of the standard eigenvalue computer programs.

## Sinusoidal Stiffness Matrices for Local Buckling in Plates

The general method described in the previous section allows for a systematic inclusion of different nonlinear terms from the strain-displacement equations; however, for most practical applications many of these terms can be neglected. For example, in the study of local instability of plates and constant cross-section thin-walled columns and panels made up of thin plates, only the nonlinear terms $(\partial u_z/\partial x)^2$ and $(\partial u_z/\partial y)^2$ need be retained, where the $z$ coordinate represents the normal direction to the plate components. Another simplification results from the thin-plate assumption $\sigma_{zz} = \sigma_{zx} = \sigma_{yz} = 0$.

The analytical solution for the deflection of plates indicates that, at instability, the buckling deformations are varying sinusoidally in the lengthwise direction.[11] This is illustrated in Fig. 2 for a channel section thin-walled column subject to a compressive axial stress. It should be noticed that the edge lines at the junctions between flat plate components remain fixed in space, and the component flats rotate about their common edge lines. Also, normal deflections on all component flats have the same wavelength. To analyze the types of structures under consideration, the cross section is divided into a series of longitudinal strips extending to infinity. Each strip can then be represented by a finite element whose length is equal to the half-wavelength $L$ of the sinusoidal deformation pattern, as illustrated in Fig. 3 where a comparison of the finite element strip representation and that of the conventional method is made.

The finite element strip is shown in Fig. 4 where for generality, in addition to the lengthwise stress $\sigma_{xx}$, the transverse stress $\sigma_{yy}$ is also included to allow for the analysis of plates or panels subjected to a biaxial stress field. Because only the out-of-plane displacements are used in the nonlinear terms, the in-plane stiffness does not affect the buckling stress. Hence, to study instability of the type of structures considered in this paper, only the out-of-plane deflections and rotations must be included in the analysis.

The normal deflection $w$ of the finite element strip can be expressed as[11]

$$u_z = w = Y(\eta) \sin(\pi x/L); \quad \eta = y/b \tag{34}$$

As an approximation for the function $Y(\eta)$, a cubic polynomial can be assumed; the coefficients in this polynomial are determined from the nodal rotations and deflections at $y = 0$ and $b$ and $x = L/2$. This leads to

$$w = \mathbf{a}(\eta) \sin(\pi x/L)\mathbf{U} \tag{35}$$

where

$$\mathbf{a}(\eta) = [(1 - 3\eta^2 + 2\eta^3)(\eta - 2\eta^2 + \eta^3)b \quad (3\eta^2 - 2\eta^3)(-\eta^2 + \eta^3)b] \tag{36}$$

$$\mathbf{u} = \{u_1 u_2 u_3 u_4\} \tag{37}$$

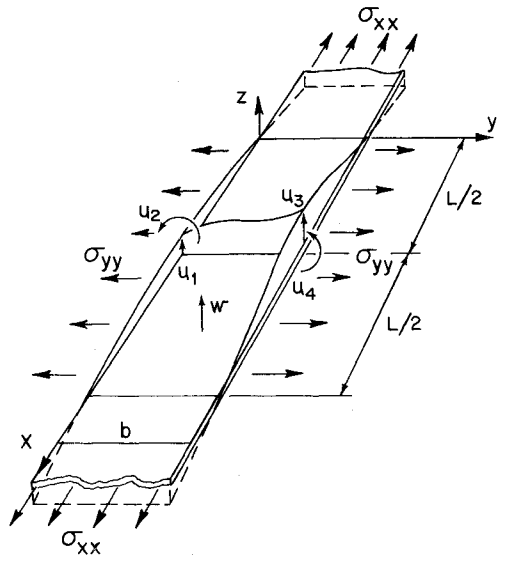


**Fig. 4 Finite element for local instability in plate structures.**

The normal and shearing linear strains can then be calculated from

$$\begin{aligned}\hat{e}_{xx} &= -z\partial^2 w/\partial x^2 = (z\pi^2/L^2)\mathbf{a}(\eta)\sin(\pi x/L)\mathbf{u}\\ \hat{e}_{yy} &= -z\partial^2 w/\partial y^2 = -(z/b^2)\mathbf{a}''(\eta)\sin(\pi x/L)\mathbf{u}\\ \hat{e}_{xy} &= -2z\partial^2 w/\partial x\,\partial y = -(2z\pi/bL)\mathbf{a}'(\eta)\cos(\pi x/L)\mathbf{u}\end{aligned} \tag{38}$$

where primes denote differentiation with respect to the non-dimensional parameter $\eta$. Collecting Eqs. (38) into a single matrix equation, it follows that

$$\hat{\mathbf{e}} = \begin{bmatrix}\hat{e}_{xx}\\ \hat{e}_{yy}\\ \hat{e}_{xy}\end{bmatrix} = z\begin{bmatrix}(\pi^2/L^2)\mathbf{a}(\eta)\sin(\pi x/L)\\ -(1/b^2)\mathbf{a}''(\eta)\sin(\pi x/L)\\ -(2\pi/bL)\mathbf{a}'(\eta)\cos(\pi x/L)\end{bmatrix}\mathbf{u} = \hat{\mathbf{b}}\mathbf{u} \tag{39}$$

The elastic out-of-plane stiffness matrix is then determined from Eq. (19). Hence

$$\mathbf{k}_E = \int_0^L\int_0^b\int_{-t/2}^{t/2}\hat{\mathbf{b}}^T\mathbf{E}\hat{\mathbf{b}}\,dx\,dy\,dz \tag{40}$$

where

$$\mathbf{E} = \frac{E}{(1-\nu^2)}\begin{bmatrix}1 & \nu & 0\\ \nu & 1 & 0\\ 0 & 0 & (1-\nu)/2\end{bmatrix} \tag{41}$$

and $E$ is the Young's modulus and $\nu$ is the Poisson's ratio. Substituting the matrix $\hat{\mathbf{b}}$ from Eq. (39) into Eq. (40) and integrating over the whole volume of the element the required elastic stiffness matrix dependent on the half-wavelength of the buckling mode is obtained, i.e.

$$\mathbf{k}_E = \mathbf{k}_{E_1}(1/L^3)+\mathbf{k}_{E_2}(1/L)+\mathbf{k}_{E_3}(L) \tag{42}$$

where

$$\mathbf{k}_{E_1}(1/L^3) = \frac{\pi^4 Ebt^3}{10{,}080(1-\nu^2)L^3}\begin{bmatrix}156 & & \text{Symmetric} & \\ 22b & 4b^2 & & \\ 54 & 13b & 156 & \\ -13b & -3b^2 & -22b & 4b^2\end{bmatrix} \tag{43}$$

$$\mathbf{k}_{E_2}(1/L) = \frac{\pi^2 Et^3}{360(1-\nu^2)bL}\begin{bmatrix}36 & & \text{Symmetric} & \\ (3+15\nu)b & 4b^2 & & \\ -36 & -3b & 36 & \\ 3b & -b^2 & -(3+15\nu)b & 4b^2\end{bmatrix} \tag{44}$$

$$\mathbf{k}_{E_3}(L) = \frac{ELt^3}{24(1-\nu^2)b^3}\begin{bmatrix}12 & & \text{Symmetric} & \\ 6b & 4b^2 & & \\ -12 & -6b & 12 & \\ 6b & 2b^2 & -6b & 4b^2\end{bmatrix} \tag{45}$$

In order to determine the out-of-plane geometrical stiffness for the element, it can be assumed that only nonlinear terms containing $u_z = w$ should be retained in the strain-displacement equation, i.e. $(\partial u_z/\partial x)^2$ and $(\partial u_z/\partial y)^2$. Furthermore, it will be assumed that stresses in the middle plane do not vary with $x$ and $y$, and that the middle plane shearing stress is zero. Denoting for convenience the nonzero middle plane stresses as $\sigma_{xx}$ and $\sigma_{yy}$, it follows from Eq. (25) that

$$\mathbf{k}_G = \sigma_{xx}\int_0^L\int_0^b\int_{-t/2}^{t/2}\mathbf{b}_{zx}{}^T\mathbf{b}_{zx}\,dx\,dy\,dz + \sigma_{yy}\int_0^L\int_0^b\int_{-t/2}^{t/2}\mathbf{b}_{zy}{}^T\mathbf{b}_{zy}\,dx\,dy\,dz \tag{46}$$

where

$$\mathbf{b}_{zx} = (\partial/\partial x)\mathbf{a}(\eta)\sin(\pi x/L) = (\pi/L)\mathbf{a}(\eta)\cos(\pi x/L) \tag{47}$$

and

$$\mathbf{b}_{zy} = (\partial/\partial y)\mathbf{a}(\eta)\sin(\pi x/L) = (1/b)\mathbf{a}'(\eta)\sin(\pi x/L) \tag{48}$$

Substituting Eqs. (47) and (48) into (46) and then integrating over the element volume, the following expression for the element geometrical stiffness matrix is obtained

$$\mathbf{k}_G = \mathbf{k}_{G_x}(1/L)+\mathbf{k}_{G_y}(L) \tag{49}$$

where

$$\mathbf{k}_{G_x}(1/L) = \frac{\sigma_{xx}\pi^2 bt}{840L}\begin{bmatrix}156 & & \text{Symmetric} & \\ 22b & 4b^2 & & \\ 54 & 13b & 156 & \\ -13b & -3b^2 & -22b & 4b^2\end{bmatrix} = \sigma_{xx}\mathbf{k}_{G_x}{}^* \tag{50}$$

$$\mathbf{k}_{G_y}(L) = \frac{\sigma_{yy}Lt}{60b}\begin{bmatrix}36 & & \text{Symmetric} & \\ 3b & 4b^2 & & \\ -36 & -3b & 36 & \\ 3b & -b^2 & -3b & 4b^2\end{bmatrix} = \sigma_{yy}\mathbf{k}_{G_y}{}^* \tag{51}$$

In Eqs. (50) and (51), $\mathbf{k}_{G_x}{}^*$ and $\mathbf{k}_{G_y}{}^*$ represent element geometrical stiffness matrices for unit values of the stresses $\sigma_{xx}$ and $\sigma_{yy}$, respectively.

Once the element stiffness matrices $\mathbf{k}_E$ and $\mathbf{k}_G$ have been determined for each element strip, the assembled cross-section stiffness matrix

$$\mathbf{K} = \mathbf{K}_E+\mathbf{K}_G = \mathbf{K}_E+\sigma_{xx}\mathbf{K}_{G_x}{}^*+\sigma_{yy}\mathbf{K}_{G_y}{}^* \tag{52}$$

is obtained from the summation of element stiffness. It should be noted that no transformation into a common (global) displacement system is required, since only normal deflections and rotations are used in the formulation of stiffnesses. The stability equation (33) can now be written as

$$\{\mathbf{K}_E+\sigma_{xx}[\mathbf{K}_{G_x}{}^*+(\sigma_{yy}/\sigma_{xx})\mathbf{K}_{G_y}{}^*]\}\mathbf{U} = \mathbf{0} \tag{53}$$

in which the stress $\sigma_{xx}$ is equivalent to the eigenvalue $\lambda$.

In Eq. (53), the matrices $\mathbf{K}_E$, $\mathbf{K}_{G_x}{}^*$ and $\mathbf{K}_{G_y}{}^*$ contain multiplying factors depending on the half-wavelength $L$. To find the buckling stress $\sigma_{xx}$ for a given stress ratio $\sigma_{yy}/\sigma_{xx}$, Eq. (53) is treated as an eigenvalue equation from which the lowest eigenvalue $\sigma_{xx}$ is determined. Since the half-wavelength $L$ is unknown, the following procedure is adopted. At first, three values of $L$ are selected: one equal to a typical width of the flat plate component of the cross section other than free edge components, and the remaining two equal to 0.9 and 0.8 of the first value. Using these three values of $L$, Eq. (53) is then solved for the lowest eigenvalue $\sigma_{xx}$. Assuming a parabolic variation of $\sigma_{xx}$ with $L$, a new value of $L$ is computed corresponding to the lowest value of $\sigma_{xx}$ on this parabola. Equation (53) is then solved again for a new $\sigma_{xx}$ corresponding to that particular value of $L$. Rejecting the value of $L$ corresponding to the highest $\sigma_{xx}$, a new parabola is constructed from which another value of $L$ is found corresponding to the lowest value of $\sigma_{xx}$. The process is repeated until desirable accuracy is obtained. In practice, it has been found that no more than five iterations are usually required.

**Table 1 Buckling stress coefficients $k$ for flat plates ($\nu = 0.3$)**

| Number of elements | Simply-supported plate | | Clamped plate | | Clamped-free plate | |
|---|---|---|---|---|---|---|
| | $N^a$ | $k$ | $N$ | $k$ | $N$ | $k$ |
| 1 | 2 | 3.62303 | 1 | 6.53097 | 2 | 1.21439 |
| 2 | 4 | 3.61574 | 3 | 6.31847 | 4 | 1.16140 |
| 3 | 6 | 3.61535 | 5 | 6.30437 | 6 | 1.15808 |
| 4 | 8 | 3.61528 | 7 | 6.30174 | 8 | 1.15748 |
| 6 | 12 | 3.61528 | 11 | 6.30075 | 12 | 1.15725 |

[a] $N$ = number of degrees of freedom

## Plate Buckling

The buckling stress for infinitely long plates of constant thickness $t$ and width $b$ is obtained from the formula

$$\sigma_x = kE(t/b)^2 \tag{54}$$

where the coefficient $k$ depends on the edge support conditions and the Poisson's ratio $\nu$. The results of computer calculations of the buckling coefficient $k$ for simply-supported, clamped, and clamped-free plates, infinitely long in the direction of the applied compressive stress $\sigma_x$, are shown in Table 1. For simply-supported and clamped plates, the condition of symmetry of the buckled mode was used in the computations. The results in Table 1 indicate clearly that only a very few elements are necessary to achieve high accuracy for the buckling stress. The number of iterations allowed in the computations was, in general, limited to five for the plate buckling analysis, as well as for all other examples described in this paper.

## Plate Buckling under Biaxial Compression

As a second example of the plate buckling analysis, the results for an infinitely long plate with edges simply-supported and subjected to a biaxial stress field are shown in Fig. 5. The results are plotted as the variation of the stress ratio $\sigma_x/\sigma_o$ with $\sigma_y/\sigma_o$ where $\sigma_o$ is the buckling stress when $\sigma_y = 0$. The computed points are for four elements and for a symmetrical mode of buckling (antisymmetrical modes give significantly higher buckling stresses and therefore are not of practical interest).

To obtain an analytical solution for this case, the solution for a simply-supported rectangular plate subjected to biaxial compression may be used. Using the results of Ref. 14, it follows that

$$\sigma_x/\sigma_o = -\lambda^2(\sigma_y/\sigma_o) + (1/4)(\lambda^2 + 2 + \lambda^{-2}) \tag{55}$$

where

$$\lambda = L/b \tag{56}$$

$$\sigma_o = [\pi^2/3(1-\nu^2)]E(t/b)^2 \tag{57}$$

$L$ is the half-wavelength, $b$ is the plate width, and $t$ is the plate thickness. For a constant stress ratio $\sigma_y/\sigma_o$, Eq. (55) can be used to determine a wavelength for which the buckling stress $\sigma_x$ is a minimum. Substitution of this wavelength into Eq. (55) leads to the following functional relationship

$$\sigma_x/\sigma_o = \tfrac{1}{2} + (\tfrac{1}{4} - \sigma_y/\sigma_o)^{1/2} \tag{58}$$

which is also plotted in Fig. 5.

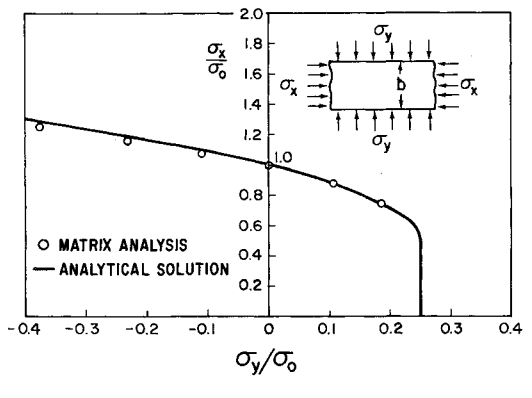


**Fig. 5 Variation of local buckling stress for biaxial stress field in an infinitely long plate with simply-supported edges.**

It is interesting to compare Eq. (58) with the solution for a single finite element. Introducing $u_2 = \theta_1$ and $u_4 = \theta_2$ with $u_1 = u_3 = 0$ and denoting compressive stresses as positive (see Fig. 5), it follows that for a single element, the equilibrium equations can be written as

$$\frac{\pi^4 Ebt^3}{10{,}800(1-\nu^2)L^3}\begin{bmatrix} 4b^2 & -3b^2 \\ -3b^2 & 4b^2 \end{bmatrix}\begin{bmatrix}\theta_1 \\ \theta_2\end{bmatrix} + \frac{\pi^2 Et^3}{360(1-\nu^2)bL}\begin{bmatrix} 4b^2 & -b^2 \\ -b^2 & 4b^2 \end{bmatrix}\begin{bmatrix}\theta_1 \\ \theta_2\end{bmatrix} + \frac{ELt^3}{24(1-\nu^2)b^3}\begin{bmatrix} 4b^2 & 2b^2 \\ 2b^2 & 4b^2 \end{bmatrix}\begin{bmatrix}\theta_1 \\ \theta_2\end{bmatrix} - \frac{\sigma_x \pi^2 bt}{840L}\begin{bmatrix} 4b^2 & -3b^2 \\ -3b^2 & 4b^2 \end{bmatrix}\begin{bmatrix}\theta_1 \\ \theta_2\end{bmatrix} - \sigma_y \frac{Lt}{60b}\begin{bmatrix} 4b^2 & -b^2 \\ -b^2 & 4b^2 \end{bmatrix}\begin{bmatrix}\theta_1 \\ \theta_2\end{bmatrix} = \begin{bmatrix}0 \\ 0\end{bmatrix} \tag{59}$$

Using the symmetry condition $\theta_2 = -\theta_1$, it can be shown readily that Eq. (59) is satisfied for $\theta_1 \neq 0$ only if

$$\frac{\sigma_x}{\sigma_o} = -\lambda^2 \frac{10}{\pi^2}\frac{\sigma_y}{\sigma_o} + \frac{1}{4}\left(\frac{120\lambda^2}{\pi^4} + \frac{20}{\pi^2} + \lambda^{-2}\right) \tag{60}$$

Comparison of Eq. (60) with Eq. (55) indicates a very close agreement between the corresponding coefficients in the two expressions. Equation (60) can now be minimized with respect to $\lambda$ and this leads to the following relationship

$$\sigma_x/\sigma_o = 5/\pi^2 + (10^{1/2}/\pi)(3/\pi^2 - \sigma_y/\sigma_o)^{1/2} \tag{61}$$

which can be compared with Eq. (58). For $(\sigma_y/\sigma_o) = 0$, Eq. (61) gives $\sigma_x/\sigma_o = 1.061565$. This means that the single element solution overestimates the exact buckling stress by 6.2%.

## Local Buckling of Thin-Walled Columns

As an example of local instability of thin-walled columns, a channel section column was analyzed. The cross section was idealized into four finite elements: two elements on one flange, and two elements on one-half of the web. The reason why only half of the total cross section was used is that the buckling mode giving the lowest stress is symmetric. Hence, only eight degrees of freedom were used in this analysis: four normal deflections and four rotations. For asymmetric sections, the complete cross section must be represented by finite elements. The results of the local instability computation are shown in Fig. 6 where the buckling coefficient $k_w$ is plotted as a function of the ratios $d/h$ and $t_w/t_f$. The buckling stress is obtained from the formula

$$\sigma_x = k_w E(t_w/h)^2 \tag{62}$$

The four-element matrix solutions are in excellent agreement with the analytical solution[15] shown in Fig. 6. It should be noted that the results for channel sections are also applicable to Z-section columns.

## Local Buckling of Stiffened Panels

### Web-Stiffened Panel

A web-stiffened panel was analyzed using a six-element idealization: two elements on the web and four elements on the skin, two on each side of the web-skin junction. Since the buckling pattern is repetitive, zero slopes (rotations) are imposed at mid points between the stiffening webs. Therefore, only eleven degrees of freedom were used: six normal deflections and five rotations. The computational results are shown in Fig. 7 where

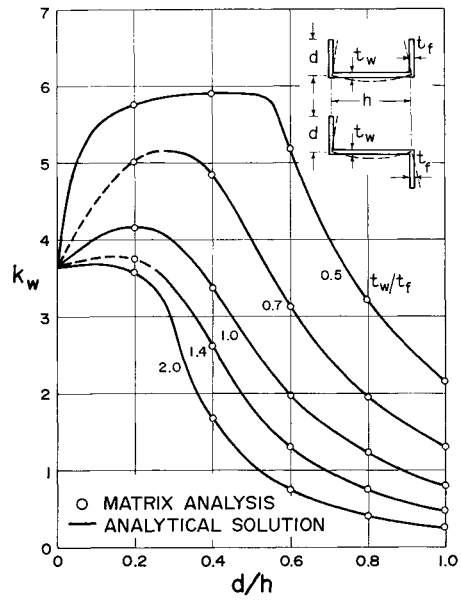


Fig. 6 Buckling coefficient for channel or $Z$-section columns ($\nu = 0.3$).

the buckling coefficient $k_s$ is plotted as a function of the ratios $d/b$ and $t_w/t_s$. The buckling stress for this case is obtained from the formula

$$\sigma_x = k_s E(t_s/b)^2 \tag{63a}$$

The analytical solution plotted in Fig. 6 was taken from Ref. 16. Here again, the agreement between the analytical and matrix results is excellent.

#### Truss-Core Sandwich Panel

To illustrate the effectiveness of the present method of determining local instability of complex configurations, a single truss-core sandwich panel was selected. Using eight elements to represent the cross section, two different local instability modes were investigated. These instability modes and the corresponding mode deflections and rotations used in the analysis are shown in Fig. 8. The analytical results[17] are presented as a carpet plot in Fig. 9, where the buckling coefficient $k_s$ is plotted as a function of the angle $\theta$ and the thickness ratio $t_c/t_s$ for $\nu = 0.3$. The buckling stress for this case is determined from

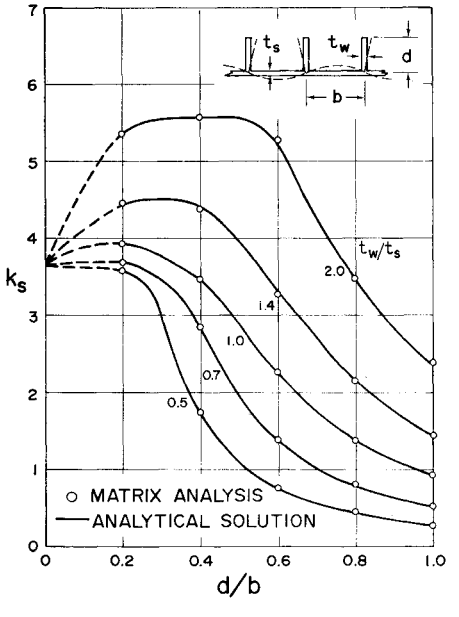


Fig. 7 Buckling coefficient for web-stiffened panels ($\nu = 0.3$).

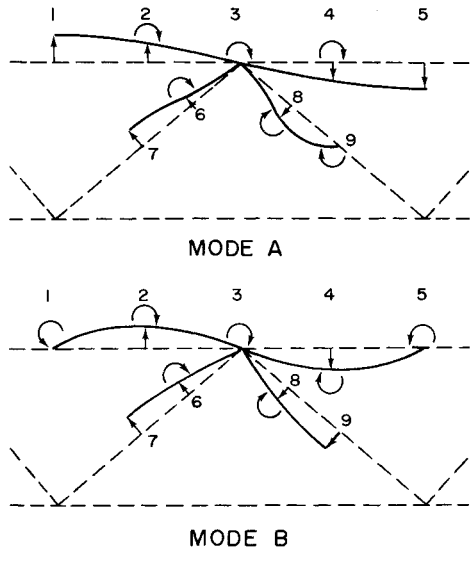


Fig. 8 Local instability modes for truss-core sandwich panels.

$$\sigma_x = k_s E(t_s/b)^2 \tag{63b}$$

There are two sets of curves for the buckling coefficient $k_s$ for the two modes, and only those parts from each set giving the lower values are shown in Fig. 9. Consequently, the plot for $k_s$ is divided into two regions: mode $A$ and mode $B$ instabilities. In mode $A$, core restrains the face skins; in mode $B$, face skins restrain the core.

## Conclusions

It has been demonstrated in this paper that the finite-element method can be effectively applied to the analysis of local instability of plates, stiffened panels, and thin-walled columns through the use of special wavelength dependent stiffness matrices. This method requires only a very few finite elements to achieve satisfactory accuracy for design purposes. The iterative solution for the buckling stress required in this method was found, in general, to be satisfactory after only five iterations. Thus, in practice the technique is very economical, and it could also be used in optimization studies of different cross-sectional configurations. The computational times on the CDC 6600 computer for a single iterative cycle (buckling stress for a given

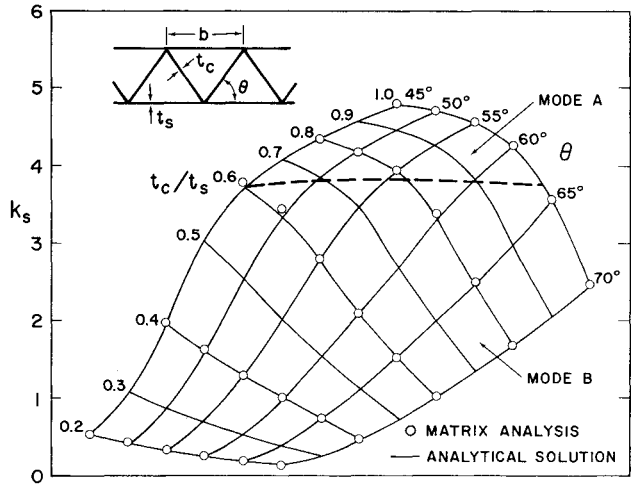


Fig. 9 Variation of the local instability stress coefficient $k_s$ with the angle $\theta$ and the thickness ratio $t_c/t_s$ for truss-core sandwich panels ($\nu = 0.3$).

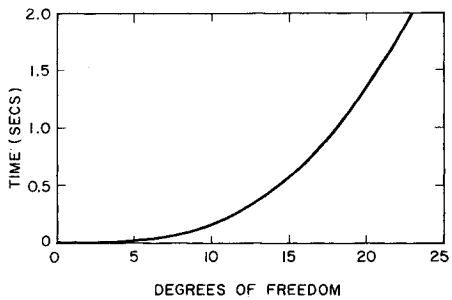


**Fig. 10 Time required to compute local buckling stress (CDC 6600 computer).**

wavelength) are shown in Fig. 10, indicating that all the results presented in this paper were computed in less than 1 sec per computation.

The concept of wavelength dependent finite-element stiffnesses employed in this paper can be extended to other applications in structural mechanics. For example, this concept has already been successfully applied in studying wave propagation in various structural components, including composites.[18] Another application could be made to a study of local vibration characteristics of stiffened panels.

## References

[1] Turner, M. J., Dill, E. H., Martin, H. C. and Melosh, R. J., "Large Deflections of Structures Subjected to Heating and External Loads," *Journal of the Aerospace Sciences*, Vol. 27, No. 2, Feb. 1960, pp. 97–106.

[2] Gallagher, R. H. and Padlog, J., "Discrete Element Approach to Structural Instability Analysis," *AIAA Journal*, Vol. 1, No. 6, June 1963, pp. 1437–1439.

[3] Wallace, C. D., "Matrix Analysis of Axisymmetric Shells Under General Loading," GAM/MC/66B-7, MS thesis, May 1966, Air Force Inst. of Technology, Wright-Patterson Air Force Base, Ohio.

[4] Martin, H. C., "On the Derivation of Stiffness Matrices for the Analysis of Large Deflection and Stability Problems," *Proceedings of the Conference on Matrix Methods in Structural Mechanics*, AFFDL TR 66-80, Nov. 1966, Wright-Patterson Air Force Base, Ohio.

[5] Kapur, K. K. and Hartz, B. J., "Stability of Plates Using the Finite Element Method," *Transactions of the ASCE, Journal of the Engineering Mechanics Division*, Vol. 92, 1966, pp. 177–195.

[6] Gallagher, R. H., Gellatly, R. A., Padlog, J. and Mallett, R. H., "A Discrete Element Procedure for Thin-Shell Instability Analysis," *AIAA Journal*, Vol. 5, No. 1, Jan. 1967, pp. 138–145.

[7] Przemieniecki, J. S., *Theory of Matrix Structural Analysis*, McGraw-Hill, New York, 1968.

[8] Przemieniecki, J. S., "Discrete Element Method for Stability Analysis of Complex Structures," *The Aeronautical Journal*, Vol. 72, No. 696, Dec. 1968, pp. 1077–1086.

[9] Navaratna, D. R., Pian, T. H. H., and Witmer, E. A., "Stability Analysis of Shells of Revolution by the Finite-Element Method," *AIAA Journal*, Vol. 6, No. 2, Feb. 1968, pp. 355–361.

[10] Gallagher, R. H. and Yang, H. T. Y., "Elastic Instability Predictions for Doubly-Curved Shells," *Proceedings of the 2nd Conference on Matrix Methods in Structural Mechanics*, AFFDL TR 68-150, Dec. 1969, Wright-Patterson Air Force Base, Ohio.

[11] Cox, H. L., "Computation of Initial Buckling Stress for Sheet-Stiffener Combinations," *Journal of the Royal Aeronautical Society*, Vol. 58, No. 525, Sept. 1954, pp. 634–638.

[12] Wittrick, W. H., "A Unified Approach to the Initial Buckling of Stiffened Panels in Compression," *The Aeronautical Quarterly*, Vol. 19, Part 3, Aug. 1968, pp. 265–283.

[13] Viswanathan, A. V., Soong, T. C., and Miller, R. E., "Buckling Analysis for Axially Compressed Flat Plates, Structural Sections, and Stiffened Plates Reinforced with Laminated Composites," CR-1887, Nov. 1971, NASA.

[14] Przemieniecki, J. S., "Buckling of Rectangular Plates under Bi-axial Compression," *Journal of the Royal Aeronautical Society*, Vol. 59, No. 536, Aug. 1955, pp. 566–568.

[15] Knoll, W. D., Fisher, G. P., and Heimerl, G. J., "Charts for the Calculation of the Critical Stress for Local Instability of Columns with *I*-, *Z*-, Channel, and Rectangular Tube Section," Advance Restricted Rept. ARR 3K.D4 (Wartime Rept. *L*-429), Nov. 1943, NACA.

[16] Boughan, R. B. and Baab, G. W., "Charts for Calculation of the Critical Compressive Stress for Local Instability of Idealized Web- and *T*-stiffened Panels," Advance Restricted Rept. ARR L4H29 (Wartime Rept. *L*-204), Aug. 1944, NACA.

[17] Anderson, M. S., "Local Instability of the Elements of a Truss-Core Sandwich Plate," TN 4292, July 1958, NACA.

[18] Talbot, R. J., "Analysis of the Dynamics of Elastic Structures by the Finite Element Method," DS/MC/72-1, Ph.D. dissertation, May 1972, Air Force Inst. of Technology, Wright-Patterson Air Force Base, Ohio.